
Site U1323¹

Expedition 308 Scientists²

Chapter contents

Background and objectives	1
Summary of operations	2
Downhole measurements	2
Figures	6
Table	13

Background and objectives

Geological setting of Mars-Ursa Basin

The geological framework of Mars-Ursa Basin is treated in detail in the “**Site U1322**” chapter. The reader is referred to this chapter regarding detailed background information and a more extensive compilation of the data available before drilling operations began. This also applies to the figures and tables contained in the chapter (see Figs. **F1**, **F2**, **F3**, **F4** in the “**Site U1322**” chapter; Table **T1** in the “**Site U1322**” chapter).

Overview of seismically mapped surfaces

Site U1323 is the middle location of the three sites drilled along an east–west transect in Ursa Basin (see Figs. **F2**, **F3** in the “**Site U1322**” chapter). Site U1323 is located in 1262 m water depth and was originally scheduled for coring, wireline logging, and logging-while-drilling/measurement-while-drilling (LWD/MWD) operations to a terminal depth (TD) of 358 meters below seafloor (mbsf), 20 m above the top of the Blue Unit (Fig. **F4** in the “**Site U1322**” chapter). The site is located within Mississippi Canyon Lease Block 898. Eight seismic surfaces are mapped along the Ursa Basin transect (Fig. **F1**; see also Fig. **F4** and Table **T1** in the “**Site U1322**” chapter). Among those, seismic Reflectors S10, S20, S30, and S80 are regional surfaces that span all three drill sites. Seismic Reflector S10 at 1731 ms two-way traveltime (TWT), or 33 mbsf, is probably the base of the hemipelagic drape sediments. Seismic Reflector S20 (1812 ms TWT; 97 mbsf) separates distal levee muds from the underlying fine-grained clastics of the eastern Southwest Pass Canyon levee. The upper and lower parts of this packet of strata seem seismically well defined, but the middle part exhibits disturbance and disruption, possibly due to slumping. Seismic Reflector S30 (1938 ms TWT; 197 mbsf) is a detachment surface that underlies one of the mass transport deposits (MTDs). Seismic Reflector S30 can be easily traced from Site U1324 farther to the west (Fig. **F4** in the “**Site U1322**” chapter). In the immediate vicinity of Site U1323 seismic Reflector S30 forms the base of a series of MTDs (Fig. **F1**). Between seismic Reflectors S30 and S50-1323 (2068 ms TWT; 305 mbsf), the reflection character is complex.

The top of the Blue Unit (seismic Reflector S80) is delineated by a weak negative polarity reflector of irregular geometry that can be traced regionally (Fig. **F1**; see also Fig. **F4** in the “**Site U1322**” chapter).

¹Expedition 308 Scientists, 2006. Site U1323. In Fleming, P.B., Behrmann, J.H., John, C.M., and the Expedition 308 Scientists, *Proc. IODP*, 308: College Station TX (Integrated Ocean Drilling Program Management International, Inc.). doi:10.2204/iodp.proc.308.107.2006
²Expedition 308 Scientists’ addresses.



Local summary of borehole expectations

Latest Pleistocene to Holocene sedimentation at Site U1323 is characterized (from youngest to oldest) by a hemipelagic drape, underlain by a packet of muddy sediments of distal levee nature, in part containing MTDs. Below this horizon, the heavily disturbed deposits of the eastern levee of Southwest Pass Canyon are in turn underlain by a body of sediments belonging to the eastern levee of Ursa Canyon, close to the core of the canyon fill. The Ursa Canyon levee deposits locally cut into the underlying sand-dominated Blue Unit (Fig. F1; see also Fig. F4 in the “Site U1322” chapter).

Drilling objectives

The primary drilling objectives at this site were the following:

- Characterize porosity and other key physical properties as a function of depth by means of correlating the LWD/MWD data with those and core observations at Sites U1322 and U1324. Derive a model to account for gradients in density/porosity and relation to overburden for the Ursa Basin transect.
- Use LWD/MWD data to optimize correlation of lithostratigraphic units between Sites U1322 and U1324 and aid development of a two-dimensional depositional and sedimentary facies model for the Ursa Basin transect.
- Monitor evolution of downhole pressure in preparation of possible future coring.

To achieve these objectives, a dedicated LWD/MWD hole (Hole U1324A) was to be drilled to a projected TD of 358 mbsf. Drilling was halted at 247 mbsf and the hole abandoned after >1.5 m sand intervals were penetrated repeatedly and because of a sudden increase in annular pressure while drilling (APWD) on the order of 150 psi at 207 mbsf. For a detailed description, see “[Operations](#).” Despite this, a complete set of LWD/MWD data was collected to TD of 247 mbsf for correlation with core, wireline logging, and LWD/MWD data from Sites U1322 and U1324.

Summary of operations

Hole U1323A

A summary of operations in Hole U1323A can be found in Table T1, and a more comprehensive description of MWD/LWD operations can be found in “[Downhole measurements](#).” A beacon was deployed at Site U1323 at 1854 h on 15 June 2005. Hole U1323A was spudded at 2025 h as the driller tagged the seafloor at 1271.0 meters below rig floor

(mbrf) (precision depth recorder = 1278.4 mbrf). The vibration-isolated television (VIT) camera was recovered and MWD drilling advanced to 206 mbsf. A sand layer, ~1.5 m in thickness (as interpreted from natural gamma ray resistance data from the MWD bit), was detected at 204 mbsf. Simultaneously, a 150 psi jump over background drilling pressure in the pressure-while-drilling (PWD) log was observed. A residual backpressure of 150 psi was also observed by the driller when he shut down the mud pumps. We pumped 50 bbl of 10.5 ppg mud in the hole and noted that the backpressure went to zero. When this mud was displaced with seawater, the overpressure returned. The pipe was filled with 110 bbl of 10.5 ppg mud and a wiper trip was made to 51.1 mbsf and back to 204.6 mbsf. The overpressure remained, and it was decided to continue to drill ahead at a very low rate of penetration (ROP), gradually increasing to 30 m/h, with “pumping and dumping” 10.5 ppg mud. At 242 mbsf, a rapid drop in gamma radiation, suggestive of a second sand interval, was observed in the data. At this point, it was decided that to maximize the amount of science and to conserve mud, we should move to the location of Site U1324 (BP Block MC 897) and plug and abandon Hole U1323A. We displaced the hole with 73 bbl of 13.5 ppg mud. The VIT camera was deployed and the top of the hole was observed to confirm that there was no flow. A free-fall funnel was deployed and inspected again with the VIT camera. We reentered Hole U1323A at 0300 h on 17 June. An obstruction or hole collapse at 140 mbsf prevented further penetration into the hole, and Hole U1323A was displaced with 31.8 bbl of 14.0 ppg cement that applied a cement plug from 140 to 40 mbsf. The drill string was then recovered, clearing the seafloor at 0550 h and the rotary table at 1010 h on 17 June.

Downhole measurements

Site U1323, located between Sites U1322 and U1324, was a dedicated LWD/MWD site. The principal objectives at this site were to characterize key physical properties and compare and correlate with Sites U1322 and U1324.

Logging while drilling and measurement while drilling

Operations

Operations in Hole U1323A used the same LWD/MWD tool configuration, bottom-hole assembly, and procedures as Site U1322 (see “[Operations](#)” in the “Site U1322” chapter). The hole was started using a rapid jet-in penetration and pump rates of ~12 strokes per minute (spm) from seafloor to ~5 mbsf

before retrieving the VIT camera. After the VIT camera was recovered, bit rotation and pump rates of 50 rpm and 12 spm were used to 25 mbsf while maintaining an ROP of 30 m/h. From 25 to 35 mbsf, pump rates were increased to 80 spm. From 35 to 247 mbsf, an ROP of 30 m/h and pump rates of at least 80 spm were maintained.

The GeoVision Resistivity tool had low battery power and would not record data when the pumps were turned off. At 198 mbsf, a 3 m thick sand layer was encountered and APWD increased by ~1 MPa. A residual backpressure of ~1 MPa was also observed by the driller when the mud pumps were shut down. We pumped 10.5 ppg mud in the hole. After a wiper trip, the overpressure stabilized and drilling operations continued. At 242 mbsf, a rapid drop in gamma radiation was observed and drilling operations were terminated to prevent penetrating an overpressured sand.

Logging data quality

Figure F2 shows the quality control logs for Hole U1323A. The target ROP of 30 m/h (± 5 m/h) was generally achieved. The density-derived caliper log is >24 cm for most of Hole U1323A, suggesting unstable borehole conditions from 0 to 130 mbsf and from 180 to 209 mbsf. These zones had an increased bulk density correction that varied from -0.15 to 0.16 g/cm³ (Fig. F2). This is greater than the larger corrections in Hole U1322A.

LWD logs were depth-shifted by identifying the gamma ray signal associated with the seafloor. The seafloor pick was 1271.1 mbrf, 0.1 m deeper than the drillers depth. The rig floor datum was located 10.5 m above sea level.

Annular pressure while drilling and equivalent circulating density

Annular pressure within the borehole was monitored during MWD operations (see discussion in “**Array Resistivity Compensated Tool**” in “Downhole measurements” in the “Methods” chapter) as annular pressure in excess of hydrostatic (APWD*) and equivalent circulating density referenced to the seafloor (ECD_{rsf}) (see “**Downhole measurements**” in the “Methods” chapter). ECD_{rsf} decreases and APWD* increases from 0 to 150 mbsf (Fig. F3). From 150 to 198 mbsf, the ECD_{rsf} log gradually increases where an overpressured silty sand interval was encountered (Fig. F3). At 198 mbsf, APWD* increased by ~1 MPa over a 3 m thick interval. After pumping weighted mud and running a wiper trip, drilling operations resumed. APWD* below 198 mbsf increased gradually. ECD_{rsf} decreased gradually, showing no significant

anomalies, thus suggesting that we did not drill through any additional overpressured units.

Results

LWD/MWD operations in Hole U1323A reached 247 mbsf. Hole diameter averaged 29.4 cm with enlarged conditions from 0 to 130 and 180 to 209 mbsf (Fig. F4). Gamma ray (GR) measurements increased with depth, averaging ~70 gAPI throughout the borehole. The GR signature showed a consistent increase from the seafloor followed by a similar decrease until reaching a low at 40 mbsf. A GR decrease to 30 gAPI indicates the presence of an overpressured sand at ~198 mbsf. At ~244 mbsf the GR values dropped to 47 gAPI, indicating the top of a second sand unit (Fig. F4).

The resistivity log showed a general increase with depth until ~198 mbsf, where a decrease in resistivity marks the top of the overpressured sand unit. Overall, resistivity ranged from 0.3 to 1.5 Ω m (mean = 1.1 Ω m). Bulk density increased gradually with depth from 1.3 to 1.9 g/cm³, corresponding to neutron porosity values ranging from 90% to 47%. Photoelectric factor (PEF) values range from 2.1×10^{-24} to 4.1×10^{-24} b/e⁻ to a depth of 184 mbsf. Below this depth, PEF increased as a result of heavy mud in the borehole. Heavy mud containing barite was used below 198 mbsf.

Interpretation of units

The stratigraphic succession drilled at Site U1323 was divided into logging Units 1, 2, and 3 based on gamma ray and resistivity logs. Logging Unit 1 is further divided into Subunits 1a, 1b, 1c, and 1d.

Logging Unit 1 (0–197 mbsf)

Logging Unit 1 is interpreted as clay with several silty intervals and two MTDs. The inferred subunits were classified using the following criteria.

Subunit 1a (0–40 mbsf)

Logging Subunit 1a extends from 0 to 40 mbsf, just below seismic Reflector S10 (Fig. F5). This subunit was defined on the basis of gamma radiation, which increases from 0 to 20 mbsf followed by a decrease until 40 mbsf. Increasing resistivity values define the base of this subunit. Subunit 1a is characterized by an alternation of low- and high-amplitude reflectors in seismic data. Subunit 1a correlates with lithostratigraphic Subunit IA at Sites U1324 and U1322. Based on the observations at Sites U1324 and U1322, this subunit is interpreted as clay with some silty intervals at the base. At Site U1322, this was inter-

preted as a hemipelagic drape and very distal turbidites from channel-levee systems to the west.

Subunit 1b (40–51 mbsf)

Logging Subunit 1b is characterized by constant gamma radiation and an increase in resistivity with two peaks corresponding to relatively high amplitude seismic reflectors within a zone of chaotic and discontinuous reflectors (Fig. F5). Based on the resistivity response and seismic character, Subunit 1b is interpreted as a 10 m thick MTD. This interpretation is linked to Sites U1322 and U1324, where reverse/normal faults and folds are observed in correlative sediments.

Subunit 1c (51–97 mbsf)

The base of logging Subunit 1c corresponds to regional seismic Reflector S20 (Fig. F5). The gamma ray profile is ~70 gAPI, resistivity increases steadily throughout the interval with minor variations, and seismic facies have parallel low- to medium-amplitude reflectors. Subunit 1c is interpreted mostly as clay and mud, based on the uniform gamma radiation and resistivity. A decrease in the gamma ray log at ~58 mbsf suggests a silt interval. In addition, this subunit has lower density than the overlying and underlying subunits (Fig. F4). This inferred subunit correlates with lithostratigraphic Subunit IC at Sites U1324 and U1322, which is composed of couplets of different-colored clay with a minor amount of silt laminae.

Subunit 1d (97–195 mbsf)

Logging Subunit 1d is based on gamma ray and resistivity data that remain fairly consistent throughout this interval. The acoustic character of the subunit is transparent or chaotic, with some isolated medium-amplitude reflections and some locally subparallel reflections toward the base of the subunit. Based on these observations, Subunit 1d is interpreted as an interval of MTDs with few silt beds. The top and bottom of Subunit 1d correspond to seismic Reflectors S20 and S30.

Logging Unit 2 (195–220 mbsf)

The top of logging Unit 2 is characterized by a sharp decrease in gamma radiation from 80 to 30 gAPI and a covariant response in resistivity. These responses are interpreted as the presence of sand units (Figs. F4, F5). The top and bottom of logging Unit 2 correspond to seismic Reflectors S30 and S40-1323. Several seismic reflectors between S30 and S40-1323 are subparallel with good lateral continuity that could represent transitions from mud/clay beds to silt/

sand-rich layers. Logging Unit 2 cannot be correlated to Site U1324 or Site U1322.

Logging Unit 3 (220–242 mbsf)

Logging Unit 3 is characterized by increasing gamma radiation with depth, which suggests an increase in mud/clay content (Figs. F4, F5). Variations are observed at ~224 mbsf, suggesting increased silt content and, at 242 mbsf, indicating increased sand content. The seismic data in this interval show discontinuous reflectors. The base of the unit is characterized by a high-amplitude reflector that correlates with sand at 242 mbsf.

Physical properties from logging data

LWD bulk density data were used to derive porosity (Equation 1 in the “Site U1321” chapter) (Fig. F6A). Bulk density increases gradually with depth from 1.3 to 1.9 g/cm³, which corresponds to porosity from 78% to 45%. The upper 40 m of the sequence (logging Subunit 1a) is characterized by relatively low bulk density that increases from 1.3 to 1.7 g/cm³ and calculated porosity from 78% to 55% (Fig. F6A). Logging Subunit 1b has small variations in bulk density and porosity. Bulk density within logging Subunit 1c gradually increases from 1.6 to 1.7 g/cm³. Logging Subunit 1d, an MTD, shows increasing bulk density from 90 to 120 mbsf and constant bulk density of 1.9 g/cm³ below 170 mbsf. Low density observed at 120 and 135 mbsf is attributed to large borehole diameter. The top of Subunit 1d is marked by a density increase of 0.02 g/cm³, whereas at the base of the subunit bulk density drops by ~0.05 g/cm³ (Fig. F6A). A comparison of LWD-calculated porosity data versus hydrostatic vertical effective stress from Sites U1322, U1323, and U1324 indicates that the sedimentary sequence drilled at the three sites follows the same trend (Fig. F6C). Thus, the data suggest that the sedimentary successions at all three sites have similar consolidation states.

Core-log-seismic integration

LWD observations are linked to seismic data through a time-depth conversion using check shot data from Hole U1324A. Reflection coefficients were calculated using the LWD density data and a constant compressional wave velocity of 1600 m/s. A 150 Hz minimum-phase Ricker wavelet was convolved with the reflection coefficients to create the synthetic seismogram (Fig. F7). The correlation between the synthetic seismogram and the high-resolution seismic matches only in the uppermost 90 mbsf. A time-depth mismatch occurs below seismic Reflector S20, where the synthetic reflections occur shallower than the same

events in the high-resolution three-dimensional seismic data (Fig. F7).

Summary

Site U1323 downhole measurements provide insights on lithofacies for correlation with Sites U1322 and U1324. Our preliminary interpretation allows for the following conclusions:

- Logging Unit 1 was interpreted to be a mud- and/or clay-banded unit with intervals of silt beds and MTDs. Chaotic intervals in seismic reflection pro-

files are interpreted as MTDs and intervals of continuous reflectors as clay.

- Logging Unit 2 is interpreted to contain silty beds and two sand beds, defined by low resistivity and gamma ray values. Seismic facies analysis suggests that these sands are associated with the Southwest Pass Canyon eastern levee.
- Logging Unit 3 was interpreted as a MTD with some silty sand beds.

Publication: 8 July 2006
MS 308-107

Figure F1. Seismic strip chart for Site U1323. Projected terminal depth (TD) and TD reached by LWD/MWD drilling (Hole U1323A) are shown. SF = seafloor.

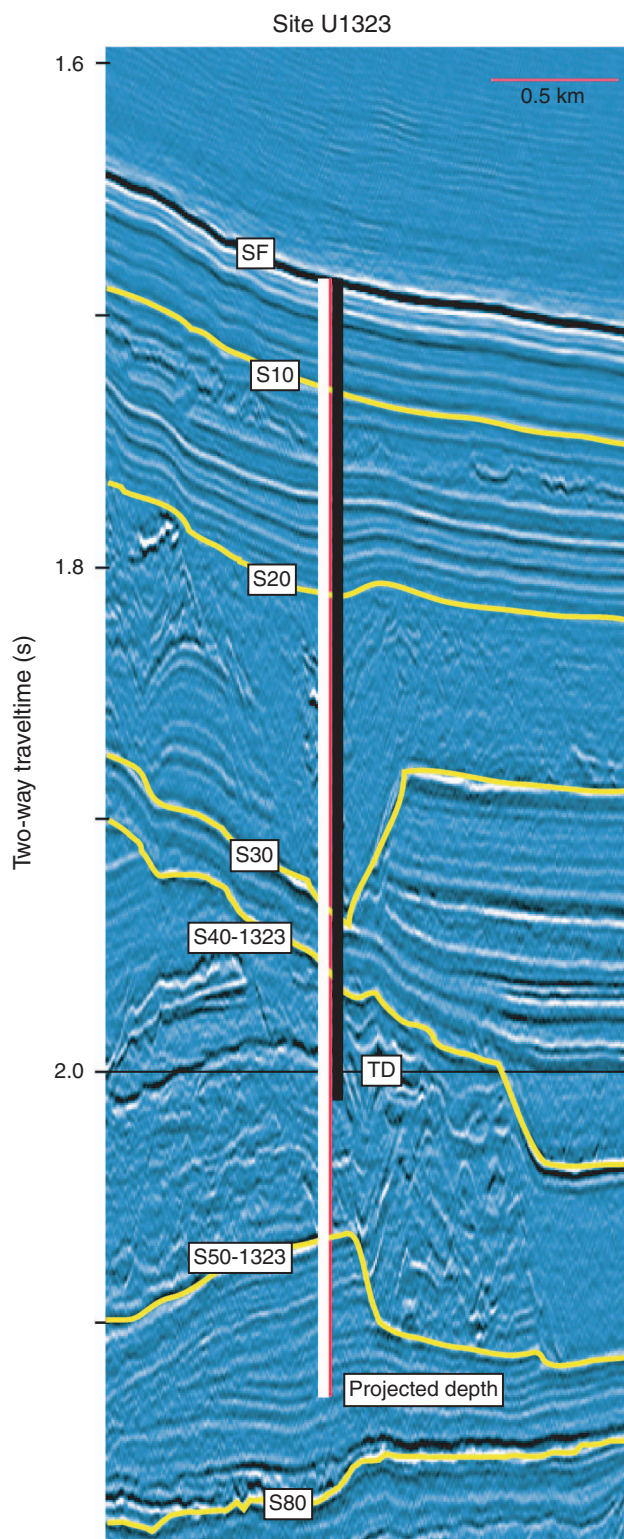


Figure F2. Data quality of curves for LWD/MWD measurements from Hole U1323A showing the rate of penetration (ROP), density-derived caliper, and density correction based on hole diameter.

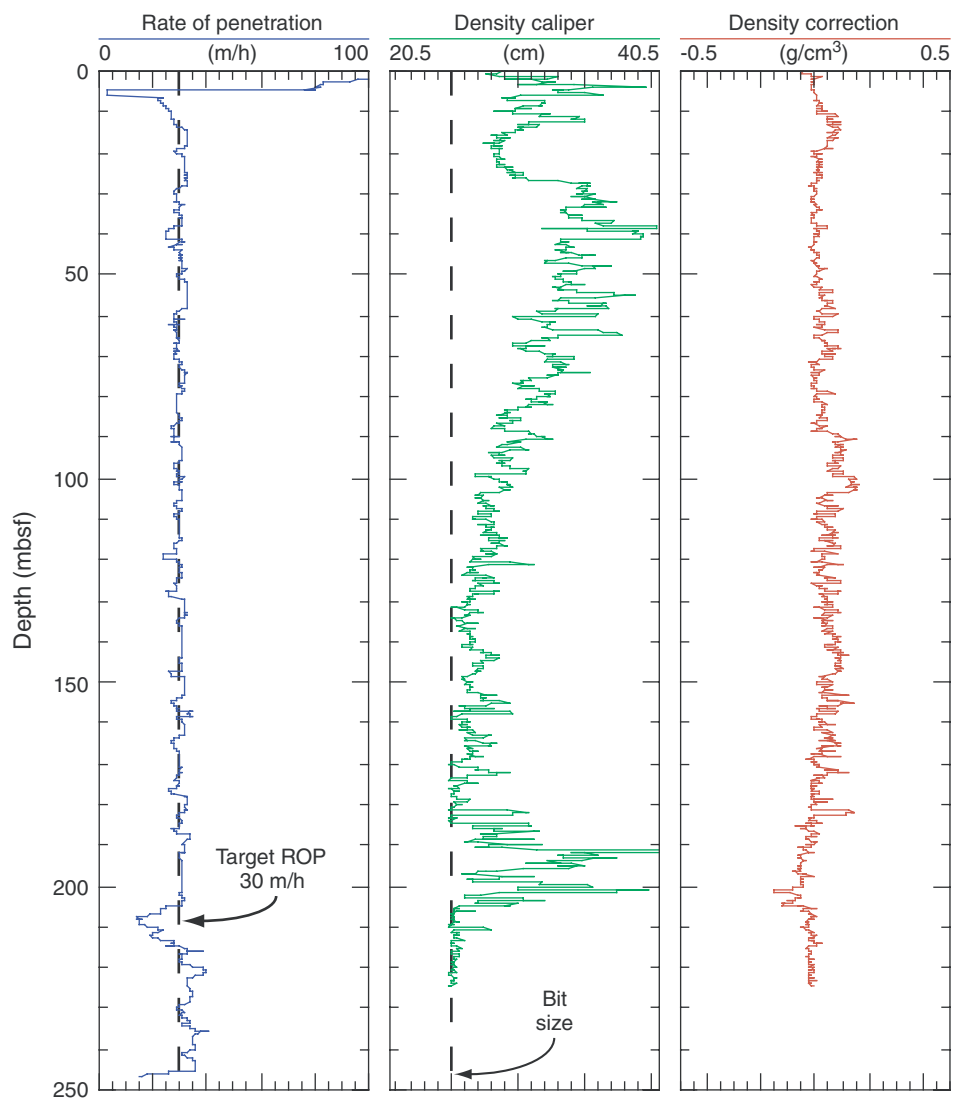


Figure F3. Annular pressure while drilling (APWD), annular pressure in excess of hydrostatic (APWD*), and equivalent circulating density referenced to the seafloor (ECD_{rsf}) in Hole U1323A. The ECD_{rsf} and APWD* curves decrease and increase, respectively, over the upper 150 mbsf. At 198 mbsf a 3 m thick sand layer recorded an increase in APWD* of ~1 MPa over the background drilling pressure. A 10.5 ppg mud was used for drilling below this point. GR = gamma radiation, SF = seafloor.

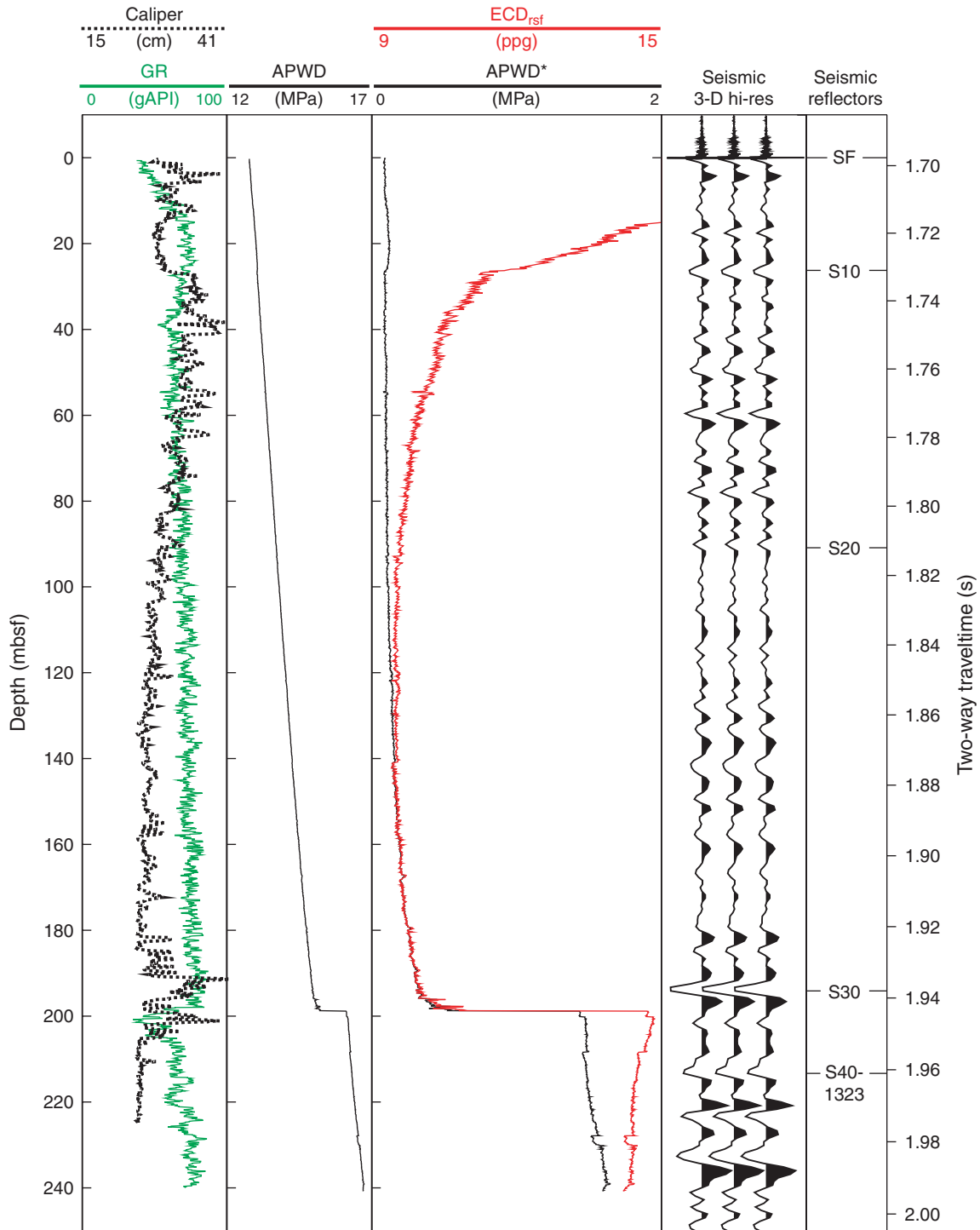




Figure F4. LWD logs recorded in Hole U1323A. Density caliper, photoelectric factor (PEF), and neutron porosity were recorded with the Vision Density Neutron (VDN) tool, whereas gamma ray and resistivity measurements were obtained with the GeoVision Resistivity (GVR) tool. Superimposed on the PEF log is a five-point average curve. Definition of units is based on gamma ray, resistivity, and seismic character. Green = zones with high resistivity, yellow = low-resistivity zones. Dashed lines = depth at which 10.5 ppg mud was used and the depth at which the VDN tool began recording heavy drilling mud flowing uphole. ARC = array resistivity compensated.

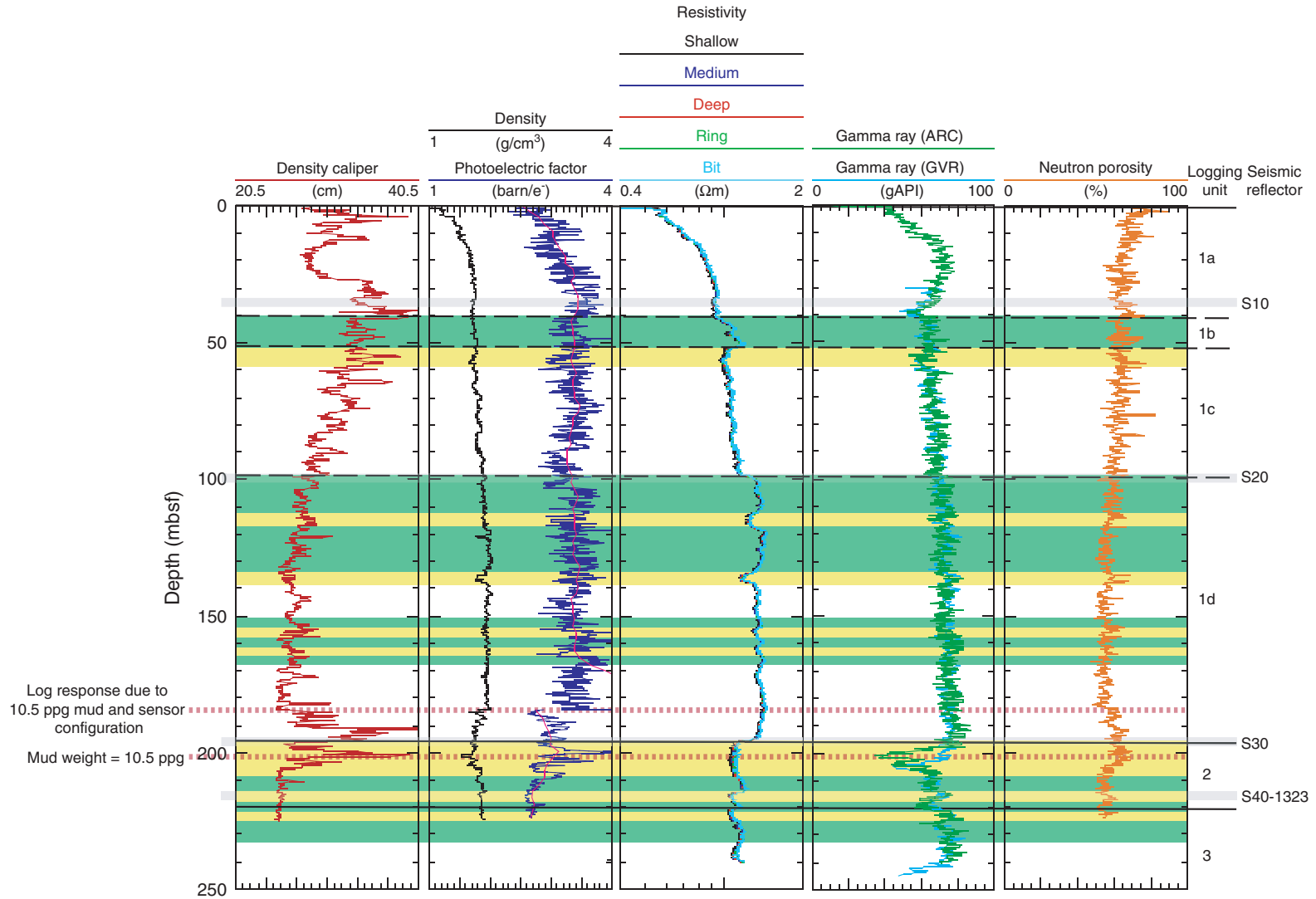


Figure F5. Seismic panel, gamma radiation, log unit/subunit divisions, inferred lithostratigraphic column, resistivity curve (log scale), and depth in two-way traveltime for Hole U1323A. The seismic panel was split at the location of Hole U1323A at trace 2170. Seismic data are approximately zero phase with black = peaks and white = troughs and plotted in depth using the check shot from Hole U1324A. Key seismic reflectors are shown in yellow and labeled (SF = seafloor). GVR = GeoVision Resistivity, ARC = array resistivity compensated.

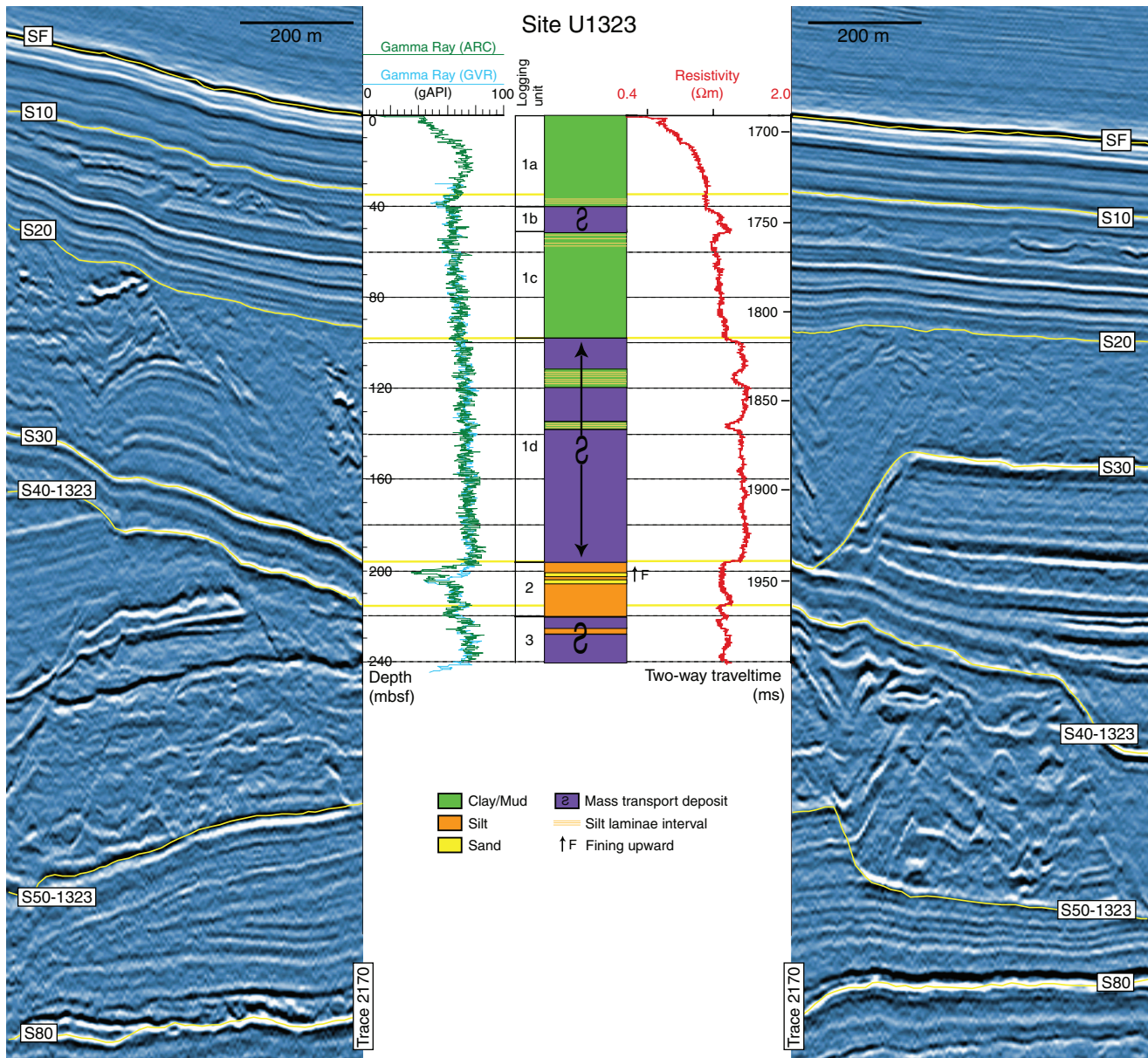




Figure F6. **A.** Bulk density and density-derived porosity from LWD data. **B.** Vertical effective stress assuming hydrostatic conditions. **C.** Porosity vs. vertical effective stress for hydrostatic conditions on a semilogarithmic diagram for all Ursa Basin sites.

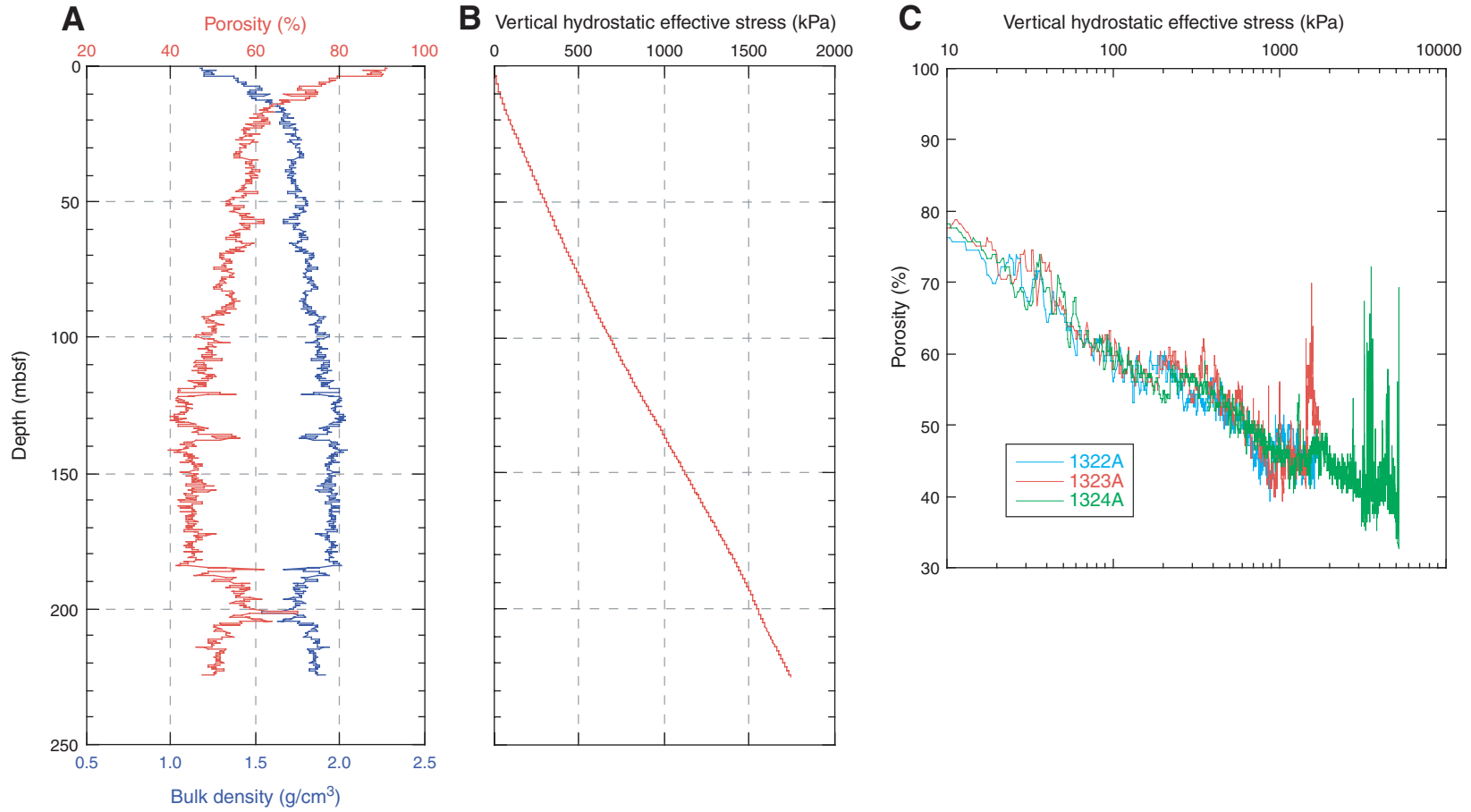


Figure F7. Log-seismic integration for Site U1323. Synthetic seismogram was constructed by convolving a 150 Hz minimum-phase Ricker wavelet with the reflection coefficient series based on LWD bulk density (not corrected for large washouts) and a constant velocity (1600 m/s). A seismic high-resolution trace (Hi-Res) is extracted from 3-D high-resolution multichannel seismic data at the location of Site U1323. GR = gamma radiation, SF = seafloor.

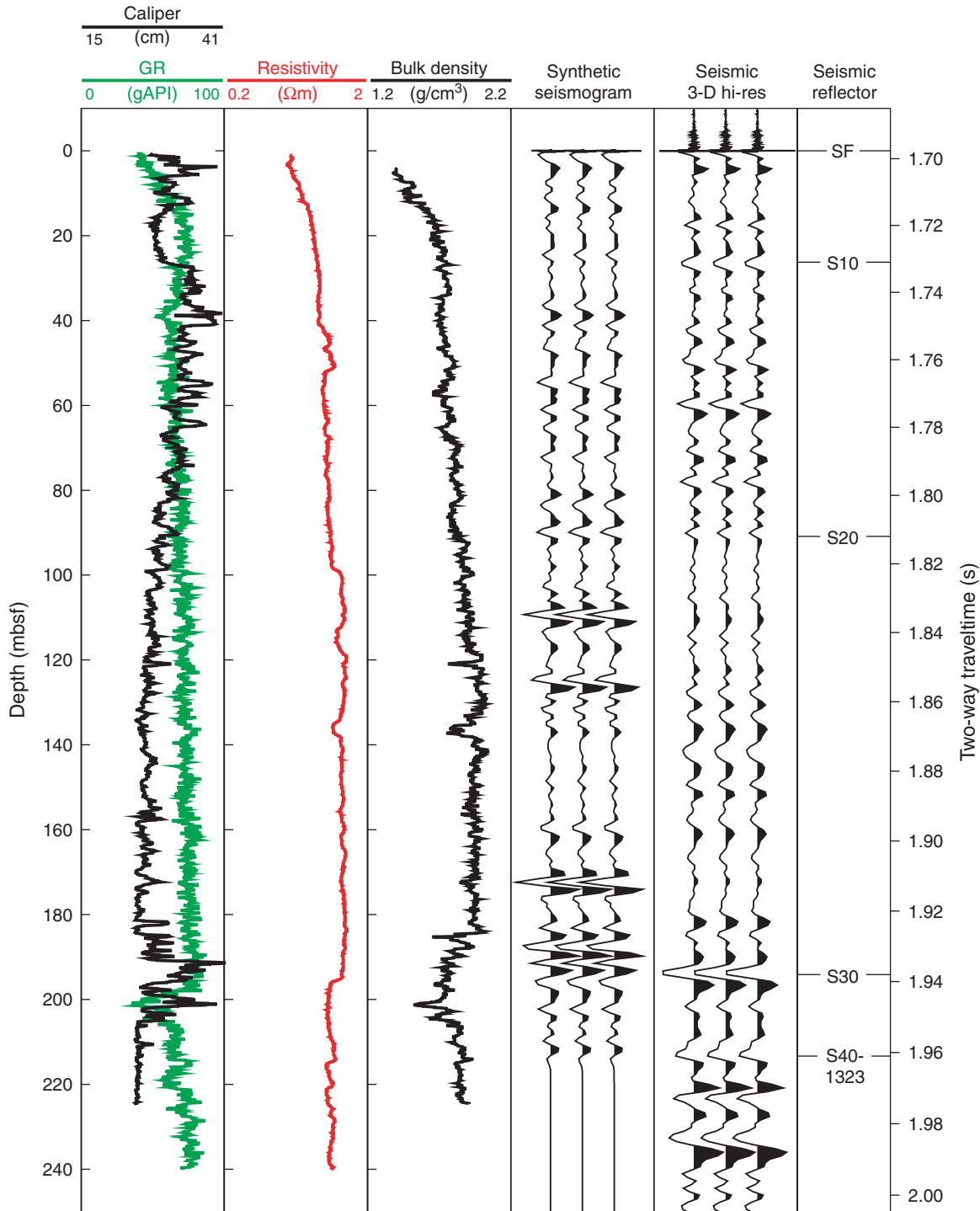


Table T1. Coring summary, Hole U1323A.

Hole U1323A

Latitude: 28°5.4725'N
 Longitude: 89°4.3509'W
 Time on site (h): 35.50
 Seafloor (drill pipe measurement from rig floor, mbrf): 1271
 Distance between rig floor and sea level (m): 10.5
 Water depth (drill pipe measurement from sea level, m): 1260.5
 Total depth (drill pipe measurement from rig floor, mbrf): 1518
 Total penetration (meters below seafloor, mbsf): 247
 Total length of cored section: 0
 Total core recovered: 0
 Core recovery (%): 0
 Total number of cores: 0

Core	Date (Jun 2005)	Local time (h)	Depth (mbsf)		Length (m)		Recovery (%)
			Top	Bottom	Cored	Recovered	
308-U1323A-							
1-0	16	1415	0	247	0	0	0
Cored totals:					0	0	0